Supplementary Information

Hybrid Polymer Dot–Magnetic Nanoparticle Based Immunoassay for Dual-Mode Multiplexed Detection of Two Mycotoxins

Yi-Chen Chen,[a†] Yu-Han Syu,[a†] Jhen-Yan Huang,[a] Chun-Yi Lin,[a] and Yang-Hsiang Chan[*abc]

[†]Authors contributed equally to this work
[a]Department of Applied Chemistry, National Yang Ming Chiao Tung University, Hsinchu, 30050, Taiwan, R.O.C.
[b]Center for Emergent Functional Matter Science, National Yang Ming Chiao Tung University, Hsinchu, 30010, Taiwan, R.O.C.
[c]Department of Medicinal and Applied Chemistry, Kaohsiung Medical University, Kaohsiung, 80708, Taiwan, R.O.C.
E-mail: Yang-Hsiang Chan (yhchan@nycu.edu.tw)

Supplementary Information

Experimental Procedures

Materials.

All reagents used in the experiment were sourced from Sigma-Aldrich, Alfa Asear, TCI, and Thermo Fisher, and were utilized as received unless otherwise stated. Highly pure water with a resistivity of 18.2 MΩ•cm was used for all experiments. he PS-PEG-COOH copolymer, consisting of a polystyrene (PS) moiety with a molecular weight (M_n) of 6500 Da and a polyethylene glycol carboxylic acid (PEG-COOH) moiety with a molecular weight of 4600 Da, and a polydispersity of 1.3, was obtained from Polymer Source (Dorval PQ, Canada) and used without any modifications. The Fe_3O_4 MNPs, modified with amino functional groups (USPIO-101) and with particle sizes ranging from 6 to 10 nm, were purchased from TANBead (Taoyuan, Taiwan). The AFB1 antibody and AFB1 conjugated with bovine serum albumin (AFB1-BSA) antigen were purchased from EastCoast Bio (MO, USA). The AFB1 antigen was obtained from FERMENTEK Ltd. The ZEN antibody and ZEN conjugated with bovine serum albumin (ZEN-BSA) antigen were purchased from Creative Diagnostics (NY, USA). ZEN, Ochratoxin A (OTA), and Deoxynivalenol (DON) were procured from Sigma-Aldrich. The AffiniPure goat anti-mouse IgG (H+L) secondary antibodies (AB_2338447) were obtained from Jackson ImmunoResearch Inc. The test strips were assembled using materials obtained from Advanced Microdevices Private Limited. These materials included nitrocellulose membranes (8 μm, CNPC), sample pads (GFB-R4), conjugate release matrices (PT-R5), and absorbent pads (AP080). The materials were cut into appropriate sizes and fitted into plastic cassettes measuring 3-6 mm. ^{1}HNMR and ^{13}CNMR spectra were recorded on Agilent VNMRS 600, Agilent 400-MR DD2 or JEOL JNM-ECZ400S/L1 spectrometers. Compound **2-3**,[1] and **4-12**[2] were synthesized according to the reported literatures.
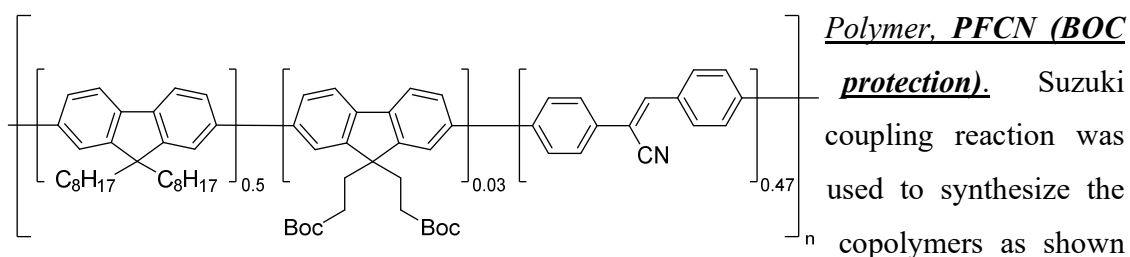
Supplementary Information

Scheme S1. Synthetic routes for the **PFCN** conjugated polymer.


PFCN
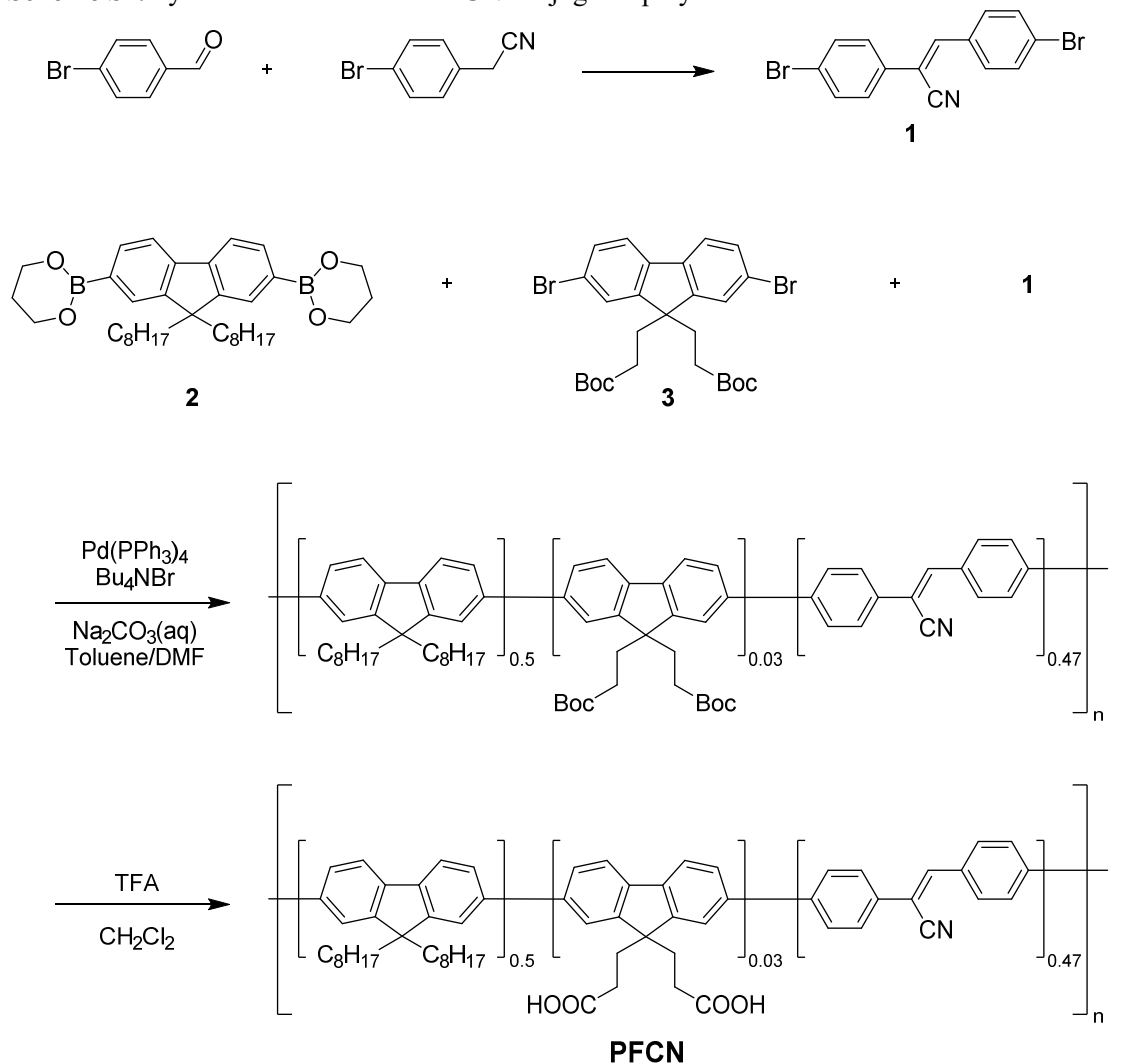
*(Z)-2,3-bis(4-bromophenyl)acrylonitrile, **1**.*[3] 4-bromobenzaldehyde (2.0 g, 10.0 mmol), 4-bromophenylacetonitrile (2.5 g, 10.0 mmol) and 20 mL of methanol were added together into a single-neck round-bottom flask, followed by the addition of sodium methoxide (1.5 mL, 25% (w/w) in methanol). Afterwards, the solution was stirred for 2 h at room temperature and then cooled in an ice-cold bath to obtain the precipitates as the crude product. The crude product was purified by column chromatography on silica gel with hexane/CH$_2$Cl$_2$ (90:10, v/v) as eluent to get 1.57 g (40%) of compound **1** as solid. ^{1}H NMR (400 MHz, CDCl$_3$) δ = 7.75 (d, J = 8.8 Hz, 2H), 7.63 – 7.56 (m, 4H), 7.54 (d, J = 8.8 Hz, 2H), 7.45 (s, 1H).

Supplementary Information

*Polymer, **PFCN (BOC protection)***. Suzuki coupling reaction was used to synthesize the copolymers as shown in Scheme S1. In a 100 mL flask, monomer **2** (34.9 mg, 0.0625 mmol), compound **1** (2.18 mg, 0.00375 mmol), and monomer **3** (21.3 mg, 0.05875 mmol) were dissolved in 2.4 mL of mixed toluene/DMF (3:1 v/v), and then 0.78 mg of tetra-n-butylammonium bromide (Bu$_4$NBr) and 0.75 mL of Na$_2$CO$_3$ (2 M) was added. The mixture solution was purged with nitrogen for 1 h. After that, the mixture solution was degassed and refilled with N$_2$ (repeated 4 times) before and after the addition of Pd(PPh$_3$)$_4$ (3.38 mg, 2.875 μmol). The reactants were stirred at 100 °C for 72 h and 5 mg of phenylboronic acid dissolved in 1 mL of THF was added. After 2 h, 0.1 mL of bromobenzene was added and further stirred for 3 h. The mixture was poured into 120 mL of cold methanol. The precipitate was filtered, washed with methanol and acetone to remove monomers, small oligomers, and inorganic salts. The crude product was dissolved in CH$_2$Cl$_2$ and then wash with water for 3 times. The organic extract was separated, dried over MgSO$_4$, and the solvent was removed under reduced pressure. The crude polymers were re-precipitated in CH$_2$Cl$_2$/methanol and washed with acetone. Finally, the product was collected by filtration to afford 20 mg of polymer **PFCN** with tert-butoxycarbonyl (Boc) protecting group.
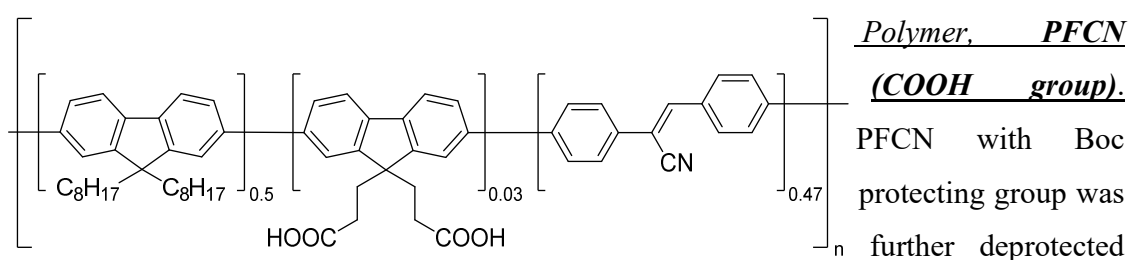

*Polymer, **PFCN (COOH group)***. PFCN with Boc protecting group was further deprotected by stirring in 10 mL of CH$_2$Cl$_2$/TFA (5:1, v/v) for 5 h at room temperature. Afterwards, the solvent was removed under reduced pressure and then CH$_2$Cl$_2$ was added to extract with brine for three times. The polymers were re-precipitated in CH$_2$Cl$_2$/methanol to obtain PFCN polymers with carboxyl functional groups.

Supplementary Information

Scheme S2. Synthetic routes for the **PFTC6FQ** conjugated polymer.

Supplementary Information

2 + 3 + 12

Pd(PPh₃)₄
Bu₄NBr
───────────→
Na₂CO₃(aq)
Toluene/DMF

TFA
───────────→
CH₂Cl₂

PFTC6FQ
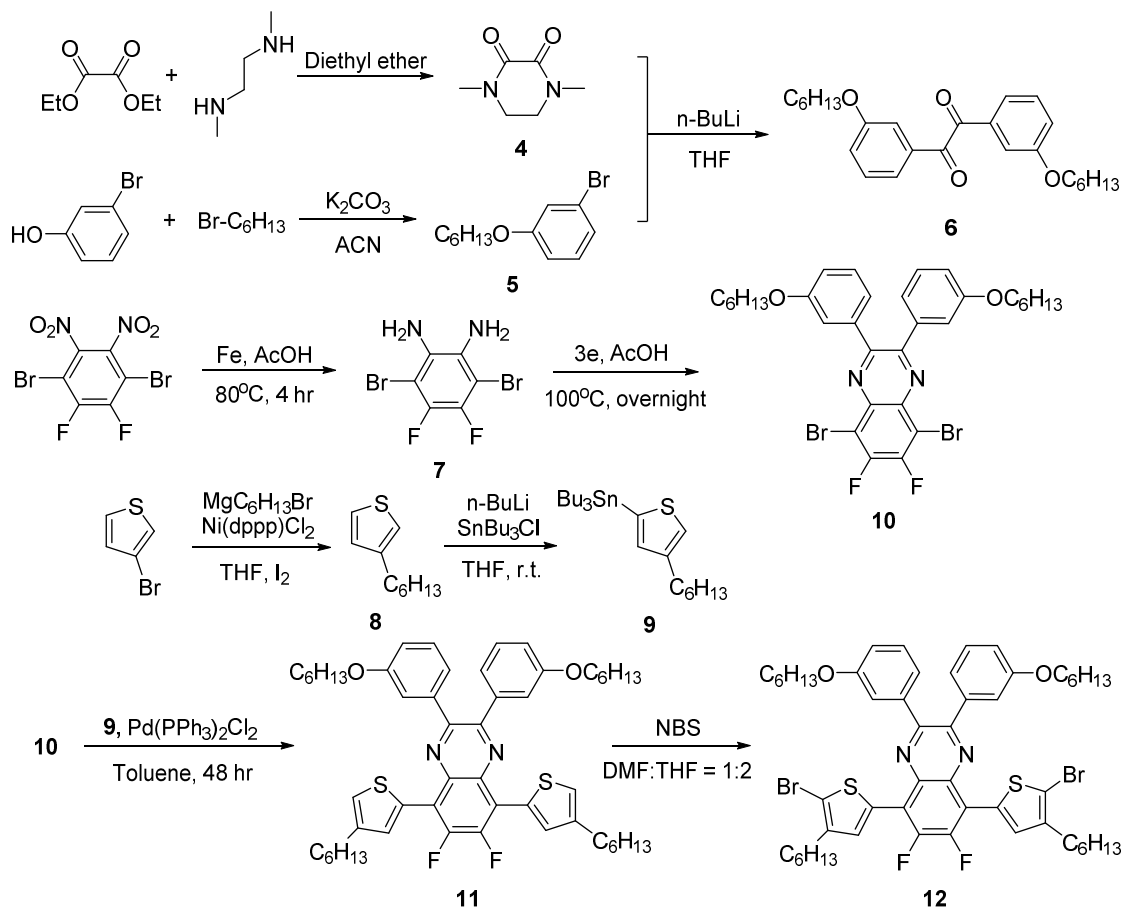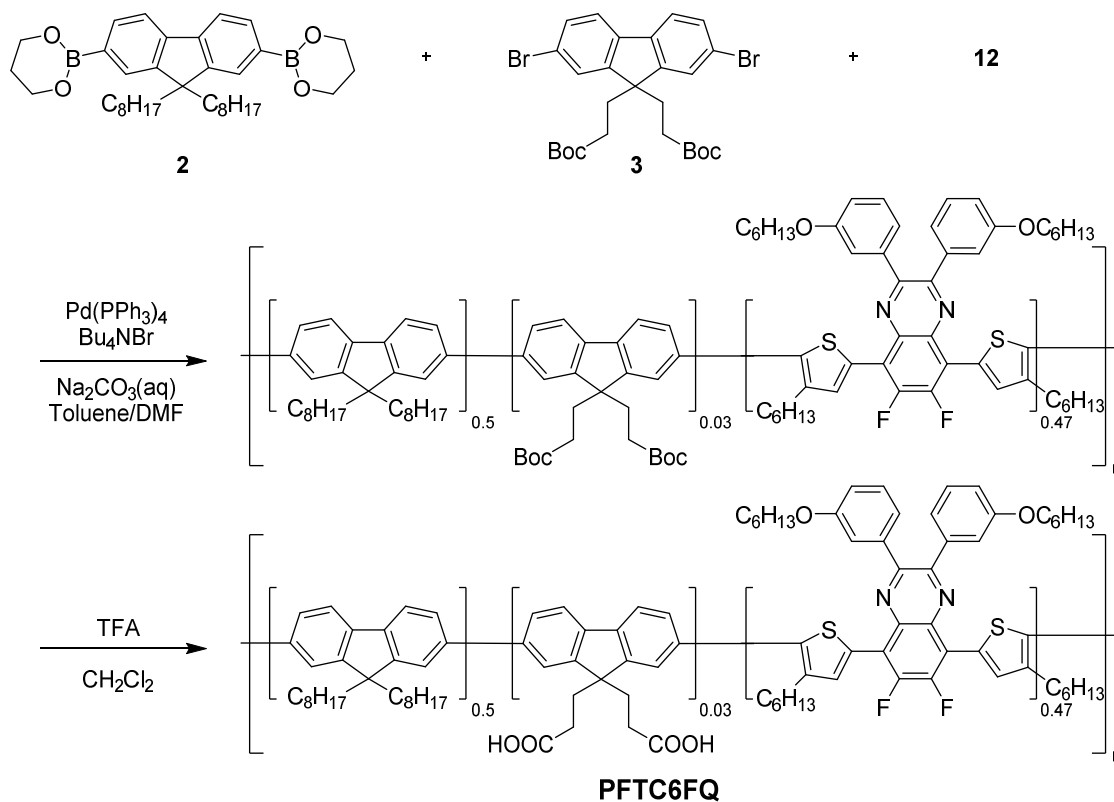
Supplementary Information

Preparation of Pdots.

To prepare PFCN Pdots with blue-green fluorescence, a mixture was prepared by combining 400 μL of PFCN (1000 ppm), 80 μL of PS-PEG-COOH (1000 ppm), and 40 μL of cumene-terminated polymer containing 75% styrene (PSMA, $M_n \sim 1900$, 1000 ppm) all in THF into a total volume of 5 mL of THF. For the preparation of PFTC6FQ Pdots with orange-red emission, 300 μL of PFTC6FQ, 40 μL of PS-PEG-COOH, and 20 μL of PSMA were used instead. The mixture was thoroughly mixed in THF and then rapidly added to 10 mL of deionized water while subjected to intense sonication. Subsequently, the THF solvent was removed by purging with nitrogen gas using a 80 °C hot plate for 45 minutes. The obtained Pdot solution was cooled to room temperature, and the final volume of approximately 8 mL was filtered through a 0.22 μm cellulose acetate syringe filter to remove any potential particle aggregates.

Preparation of MNP@PFCN and MNP@PFTC6FQ.

1 mL of MNP solution (0.3 mg/mL) was combined with 14 mL of poly(sodium 4-styrenesulfonate) (PSS, 5% w/w in 1 M Na_2SO_4) and the mixture was stirred at a speed of 500 rpm for 1 h. Following this, the solution underwent centrifugation at 14,000 rpm for 10 min, and the supernatant was discarded. Next, 1 mL of deionized water was added, followed by the addition of 14 μL of cetyltrimethylammonium bromide (CTAB, 0.1 M). The mixture was stirred at 500 rpm for 1 hour and then subjected to centrifugation at 14,000 rpm for 10 minutes. The resulting pellet was re-suspended in 1 mL of deionized water to obtain PSS/CTAB coated MNPs. For the subsequent coating PFCN or PFTC6FQ Pdots onto the surface of PSS/CTAB coated MNPs, a mixture containing 2 mL of PFCN or

Supplementary Information

TC6FQ Pdot solution, 1 mL of PSS/CTAB coated MNP solution, and 750 mL of 10 mM PBS buffer (pH = 7.4) was prepared in a vial and stirred at 65 °C for 1 h. After the coating process, the solution was centrifuged at 14,000 rpm for 10 min. The supernatant was then discarded, and the precipitate was re-suspended in 1 mL of deionized water, resulting in the formation of MNP@Pdot nanohybrids.

Antibody Conjugation of MNP@PFCN and MNP@PFTC6FQ.

To functionalize the surface of ZEN antibodies, a vial was prepared by adding 1 mL of MNP@PFCN, 20 μL of 5% (w/w) PEG (Mn = 3350), 20 μL of 1M HEPES buffer, 20 μL of freshly prepared 1-ethyl-3-(3-dimethylaminopropyl)carbodiimide (EDC, 5 μg/mL), 5 μL of *n*-hydroxysuccinimide (NHS, 5 μg/mL), and 70 μL of ZEN antibodies (0.1 mg/mL). The mixture was then allowed to react at room temperature for 4 h. After the reaction, the solution was centrifuged at 14,000 rpm to remove the supernatant. The resulting pellet was collected and resuspended in 100 μL of pure water, resulting in the formation of MNP@PFCN nanohybrids. For the preparation of MNP@PFTC6FQ, PFTC6FQ and AFB$_1$ antibodies were used in place of PFCN and ZEN antibodies, respectively.

Fabrication of Test Strip by Using MNP@Pdot-Antibody Probes.

Scheme 1 depicts the workflow for the detection processes, including the assembly and arrangement of test strips. The absorbent pad, sample pad, and nitrocellulose membrane were all trimmed to a square shape measuring 6 millimeters in length and 3 millimeters in width. Prior to the assembly, the sample pad was modified by 2% Triton X-100 and 2% PEG in 20 mM HEPES buffer for 1 h to reduce the non-specific adsorption of probes,

Supplementary Information

followed by drying under vacuum for 4 h. To fabricate the nitrocellulose membrane, an automated lateral flow reagent dispenser (RP-1000, Regabio, Taiwan) was utilized. The membrane consisted of a test line containing either ZEN-BSA (1 mg/mL) or AFB1-BSA (1 mg/mL) antigens, as well as a control line comprising IgG secondary antibodies (0.3 mg/mL). The test line was 3 millimeters wide. To enable multiplexed detection, both ZEN-BSA and AFB$_1$-BSA detection antigens were loaded onto the test line simultaneously. Subsequently, the test strip was subjected to a vacuum environment for a duration of 3 min to ensure water was completely dried. After the fabrication of the test and control lines, the nitrocellulose membrane was assembled into a test strip by attaching the absorbent pad and sample pad. Lastly, the 3-6 mm plastic cassette was used to fit the test strip.

Detection of ZEN/AFB$_1$ by MNP@Pdot-Based ICTS.

To prepare the running buffer, a mixture of various substances was combined. Specifically, 5 µL of 5% (w/w) Triton X-100, 10 µL of 1% (w/w) glycerol, 5 µL of 5% (w/w) polyethylene glycol 3000, and 5 µL of 5% (w/w) sucrose were mixed together. Additionally, 10 µL of MNP@Pdot probes, X µL of the target solution containing ZEN and/or AFB$_1$, and (65-X) µL of 20 mM HEPES buffer were added to the mixture. For the calibration samples used to establish the calibration curves, ZEN/AFB$_1$/OTA/DON were spiked into the running buffer. Volumes ranging from 0 to 20 µL of the spiked solution were added to the running buffer, resulting in a final volume of 0.1 mL. Initially, negatively charged polyelectrolyte PSS was utilized to encapsulate amine-functional MNPs, which were later coated with positively charged CTAB. PFTC6FQ and PFCN conjugated polymers were synthesized separately and transformed into Pdots through a

Supplementary Information

nanoprecipitation method. These Pdots were subsequently used to cap the MNPs, resulting in hybrid nanomaterials known as MNP@Pdots. To enable the detection of specific antigens, AFB$_1$ or ZEN detection antibodies were linked to the MNP@Pdots. The nitrocellulose membrane featured a test line that contained AFB$_1$ or ZEN antigens, as well as a control line comprising IgG secondary antibodies. By visually inspecting the color shade or fluorescence intensity of the test line, the presence of the target antigens could be detected with the naked eye. Alternatively, for quantitative analysis, the magnetic signals on the control and test lines could be measured using a magnetic assay reader. This provided a means of accurately determining the concentration of the target antigens. When analyzing local food samples from Taiwan, the standard method of testing for mycotoxins in food regulated by the Taiwan Food and Drug Administration was followed.[4] In order to accommodate the detection linear range of the mycotoxin calibration curve, it is necessary to properly dilute certain food samples. After loading the samples, the test strips were left undisturbed for a duration of 10-15 min until the results became visible. The fluorescence images of the test strips can be captured using a regular digital camera (e.g., Nikon Z7II) or a smartphone under a handheld 365 nm UV lamp (model: UVG-11, 4w, VWR International, LLC.). The camera setting is: 1) F-stop: f/3.5; 2) Exposure time: 1/2-1/8 s; 3) ISO speed: ISO-500; 4) Exposure bias: -1 step; 5) Focal length: 18 mm; 6) Max aperture: 3.6; 7) Metering mode: Multi-zone; 8) Flash mode: No flash; 9) 35 mm focal length: 27; 10) Color temperature: 4000 K. Subsequently, these images were processed using ImageJ with Java to measure the fluorescence ratios between the control and test lines. To measure magnetic signals, a magnetic assay reader (Magna Bioscience LLC, San Diego, CA, USA) was employed. The magnitude of the magnetic signal captured is in

Supplementary Information

direct correlation with the quantity of magnetic material present in the assay reaction line, and it is presented in terms of relative magnetic units (RMU). To reduce instrument variability, RMU signals undergo normalization protocols, yielding a magnetic assay reader (MAR) value that serves as the basis for all presented data.[5] Each dataset was subjected to at least three repeated measurements.

Characterization of MNP@Pdots.

The UV-visible absorption spectra of the produced nanohybrids were examined using a Dynamica Halo DB20S UV-visible spectrometer from Dynamica Scientific. The average hydrodynamic radius was measured using a Malvern Zetasizer Nano S, which employed dynamic light scattering (DLS) technique. For transmission electron microscopy (TEM) analysis of the synthesized Pdots, a Hitachi HT7700 transmission electron microscope operating at an acceleration voltage of 100 kV was utilized. To prepare the TEM sample, a carefully measured 7 µL of diluted MNP@Pdot aqueous solution was dropped onto a carbon-coated grid and allowed to dry for 24 h. The grid was then subjected to an additional 12 h of drying at 60 °C in an oven to ensure complete evaporation of water. Fluorescence spectra were recorded using an F7000 spectrofluorometer from Hitachi High-Tech Corporation.

Data Availability.

The main data supporting the findings of this study are available within the article, as well as the Supplementary Information file. Should any raw data files be needed in another format they are available from the corresponding author upon reasonable request.

Supplementary Information

Results and Discussion

Our objective was to develop a dual-readout ICTS capable of magnetic and fluorescent detection, enabling the simultaneous identification of ZEN and AFB$_1$ in real samples. We anticipated observing a distinct color variation on the test line upon the detection of ZEN, AFB$_1$, or both, using fluorescence as the indicator. These qualitative results provided a convenient means of detecting the presence of these mycotoxins, facilitating rapid food safety assessment. Moreover, the magnetic signals obtained from the test strip could be employed for quantitative analysis, allowing for the precise determination of the target mycotoxins. This enhanced the efficiency of mycotoxin screening, contributing to the assurance of food safety standards.
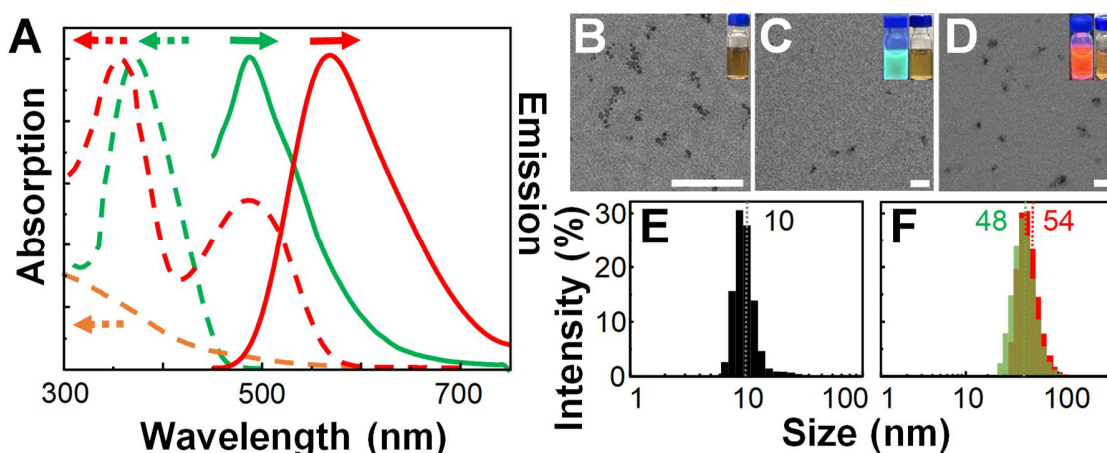
Figure S1. (A) Absorption spectra of MNPs (dashed brown line), MNP@PFTC6FQ (dashed red line), and MNP@PFCN (dashed green line) nanohybrids in aqueous solutions; and fluorescence spectra of MNP@PFTC6FQ (solid red line) and MNP@PFCN (solid green line) in water. (B) TEM images of MNPs. The inset in the right-upper image shows the photograph of MNPs. (C) TEM images of MNP@PFCN nanoparticles. The right-upper image includes an inset photograph of MNP@PFCN under both ambient (right) and UV (left) light conditions. (D) TEM images of MNP@PFTC6FQ nanoparticles. The right-upper image includes an inset photograph of MNP@PFTC6FQ under both ambient (right) and UV (left) light conditions. The scale bars in B-D correspond to 50 nm. (E) Hydrodynamic diameters of MNPs determined using DLS, with the average size indicated by the number. (F) Hydrodynamic diameters of MNP@PFCN (green histogram) and MNP@PFTC6FQ (red histogram) acquired from DLS, with the average sizes indicated by the numbers.

Supplementary Information

Scheme 1 demonstrates the preparation process for the synthesis of negatively charged Pdots (ζ = -32 to -34 mV). This involved the rapid injection of a THF solution containing PFTC6FQ/PFCN polymers into pure water, utilizing a nanoprecipitation technique. The surfaces of positively charged MNPs (with a ζ potential of +41.6 mV) were first coated with a negatively charged polyelectrolyte, PSS, to passivate the function of amine groups, which could potentially cross-conjugate with antibodies or nonspecifically adsorb onto the nitrocellulose membrane of the test strip. After the coating of PSS, the zeta potential of MNPs turned from +41.6 mV to -55.3 mV (Figure S2). We then inserted the second adhesive layer, positively charged CTAB, on the surfaces of PSS-coated MNPs with a ζ potential of +31.5 mV. Subsequently, the Pdots were utilized to entrap MNPs as the outermost layer with the resulting ζ potentials of -25 and -28 mV for MNP@PFCN and MNP@PFTC6FQ nanohybrids, respectively (Figure S2). The amount coating layers on MNPs were optimized in an effort to deactivate the effect of amines while preserving the magnetic signals of MNPs. The magnetic intensities remained at over 50 % after three layers of coating, sufficient for quantitative measurements. (Figure S3). The MNP@Pdot that obtained from this work exhibited a combination of benefits from both MNPs (magnetic signals that are unaffected by interference in food samples) and Pdots (extremely bright fluorescence). These nanohybrids offer excellent characteristics for dual-readout platforms, combining magnetic and fluorescent capabilities.
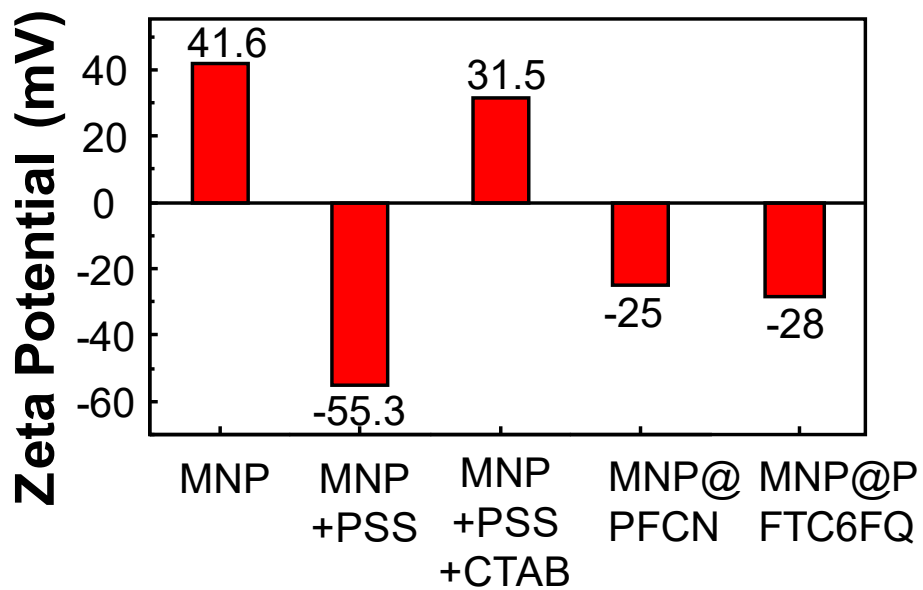
Supplementary Information

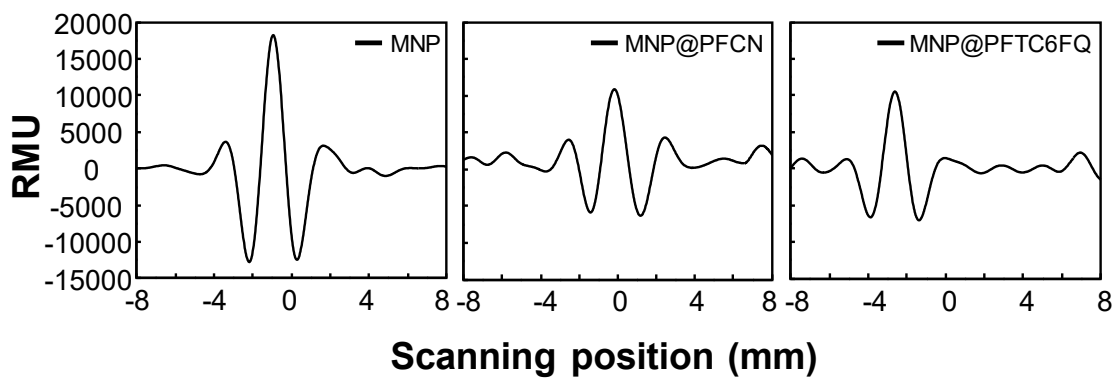**Figure S2.** Zeta potentials of MNP probes after coating with different materials.

Figure S3. Magnetic intensities of bare MNPs (left column), MNP@PFCN (middle column), and MNP@PFTC6FQ probes (right column).
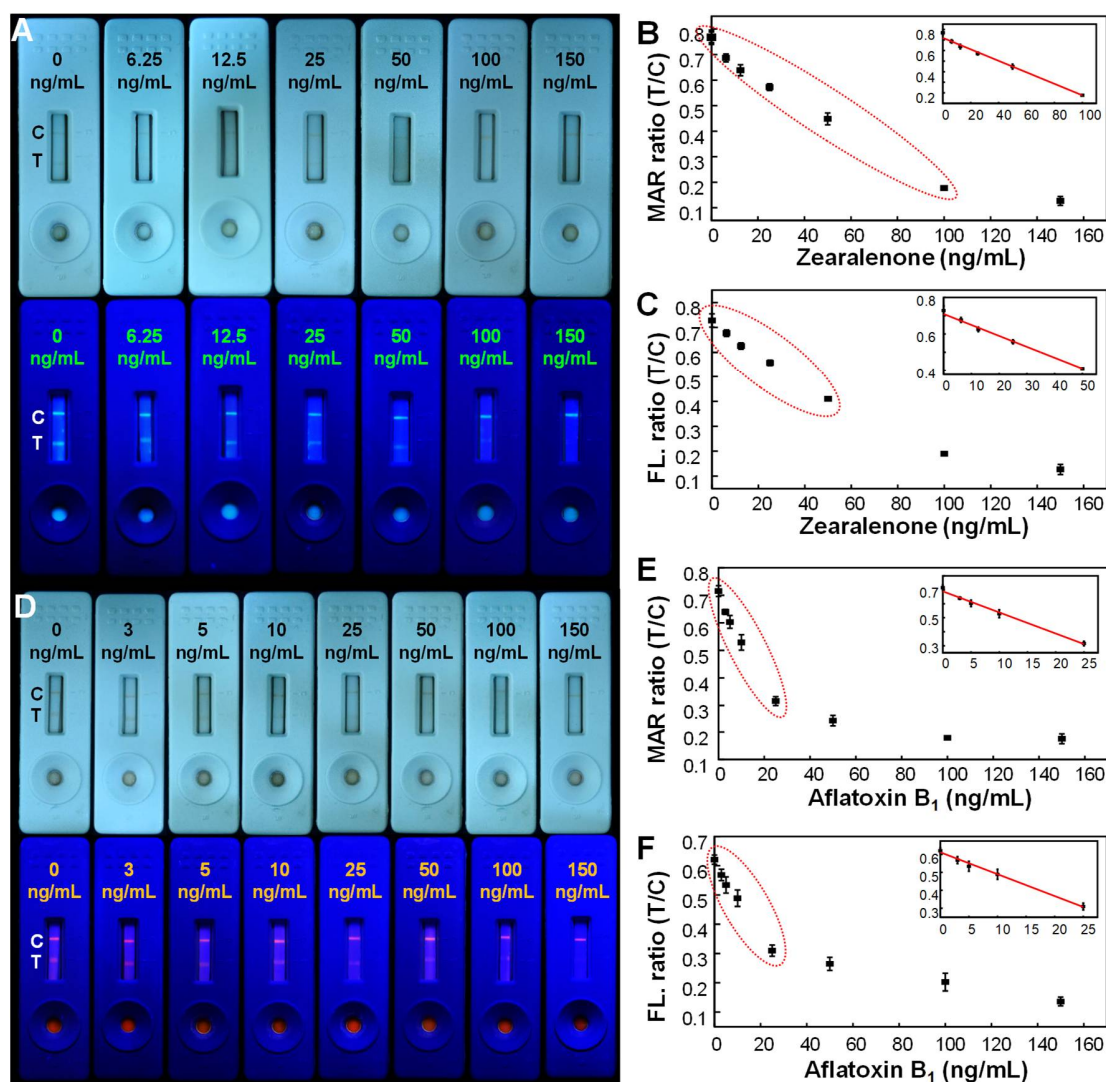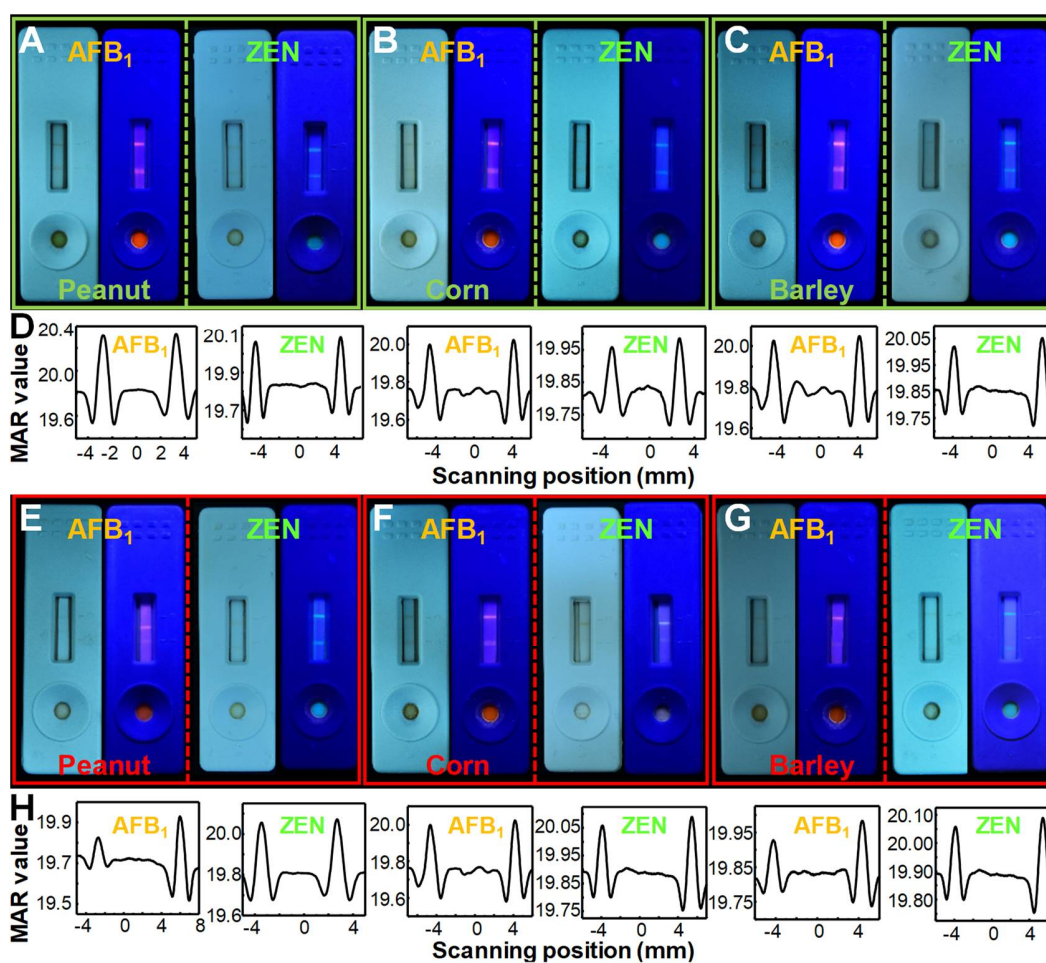
Supplementary Information

Figure S4. Quantitative analysis of ZEN and AFB_1 by MNP@Pdots-based ICTS. (A) Photographs of the test strips taken under ambient conditions (upper panel) and 365 nm light irradiation (bottom panel) after their application to samples containing ZEN concentrations ranging from 0 to 150 ng/mL. The MNP@PFCN probes were utilized for this experiment. Their corresponding detection dynamic ranges of ZEN based on (B) magnetic signals and (C) fluorescence signals. (D) Photographs of test strips were taken after applying them to samples containing AFB_1 ranging from 0 to 150 ng/mL, both under ambient conditions (upper panel) and 365 nm light irradiation (bottom panel). The MNP@PFTC6FQ probes were utilized for this experiment. Their corresponding detection dynamic ranges of AFB_1 based on (E) magnetic signals and (F) fluorescence signals. The insets in each panel display the corresponding calibration curves.

For the evaluation of detection selectivity towards ZEN by using MNP@PFCN probes, the test line was engineered with ZEN antigens (Figure S4A). Likewise, only AFB_1 antigens were decorated on the test line by using MNP@PFTC6FQ probes (Figure S4D).

Supplementary Information

It was evident that the color depth was not very conducive to recognition. Conversely, there was a noticeable decrease in fluorescence brightness intensity as the concentrations of ZEN/AFB$_1$ increased. Furthermore, we discovered that the linear range and sensitivity (as represented by the slope of the calibration curve) derived from magnetic signals (Figure S4B) appeared to be better than those obtained from fluorescence signals (Figure S4C). This once again validated that magnetic signals are better suited for quantitative measurements, while fluorescence signals are suitable for rapid qualitative determination. This fact can be partially attributed to the fluorescence interference from several types of aflatoxins,[6] leading to the decreased sensitivity of fluorometric method. The same situation was observed for AFB$_1$ when utilizing MNP@PFTC6FQ probes. (Figure S4E-F).

Supplementary Information

Figure S5. Quantitative analysis of real samples. Fresh (A) peanut, (B) corn, and (C) barley purchased from a local supermarket analyzed by MNP@Pdot-based test strips. The photographs' left sides depict the test results obtained under room light, whereas their right sides reveal the fluorescence observed under 365 nm UV light. Their corresponding magnetic signals are shown in (D). Stale (E) peanut, (F) corn, and (G) barley stored for 3 months and then analyzed by MNP@Pdot-based test strips. The photographs' left sides depict the test results obtained under room light, whereas their right sides reveal the fluorescence observed under 365 nm UV light. Their corresponding magnetic signals are shown in (H).

Table S1. Concentrations of AFB_1 and ZEN in Real Samples Determined by MNP@Pdot-based Test Strip and HPLC.

	Test Strip (ng/mL)		HPLC (ng/mL)	
	AFB_1	ZEN	AFB_1	
				ZEN
Fresh Peanut	ND[a]	ND	ND	ND
Fresh Corn	ND	b	ND	1.93
Fresh Barley	ND	b	ND	3.78
Stale Peanut	19.95	ND	17.15	ND
Stale Corn	3.95	18.59	4.04	19.07
Stale Barley	6.62	11.19	8.87	11.18

[a]ND: not detected [b]Below the detection limit of the test strip

To evaluate the practicability of this MNP@Pdot-based ICTS platform in real samples, we chose peanut, corn, and barley obtained from nearby supermarkets, and then stored a portion of them in darkness for a duration of 3 months. These three samples were chosen because they have varying concentrations of ZEN and AFB_1. Next, we employed MNP@Pdot-based test strips to measure the concentrations of ZEN and AFB_1 in both fresh and aged samples. The results were shown in Figure S5A-C whereas vibrant fluorescence could be observed on the test lines test lines for fresh samples. Based on the quantitative analysis of magnetic signals portrayed in Figure S5D, the ZEN and AFB_1 levels fall below the test strips' detection threshold. Significant reductions in fluorescence were detected on the test lines of stale samples to varying degrees, indicating distinguishable levels of ZEN or AFB1 present in the samples. Subsequently, we compared the quantitative outcomes attained from the test strips with those obtained through the standard HPLC method
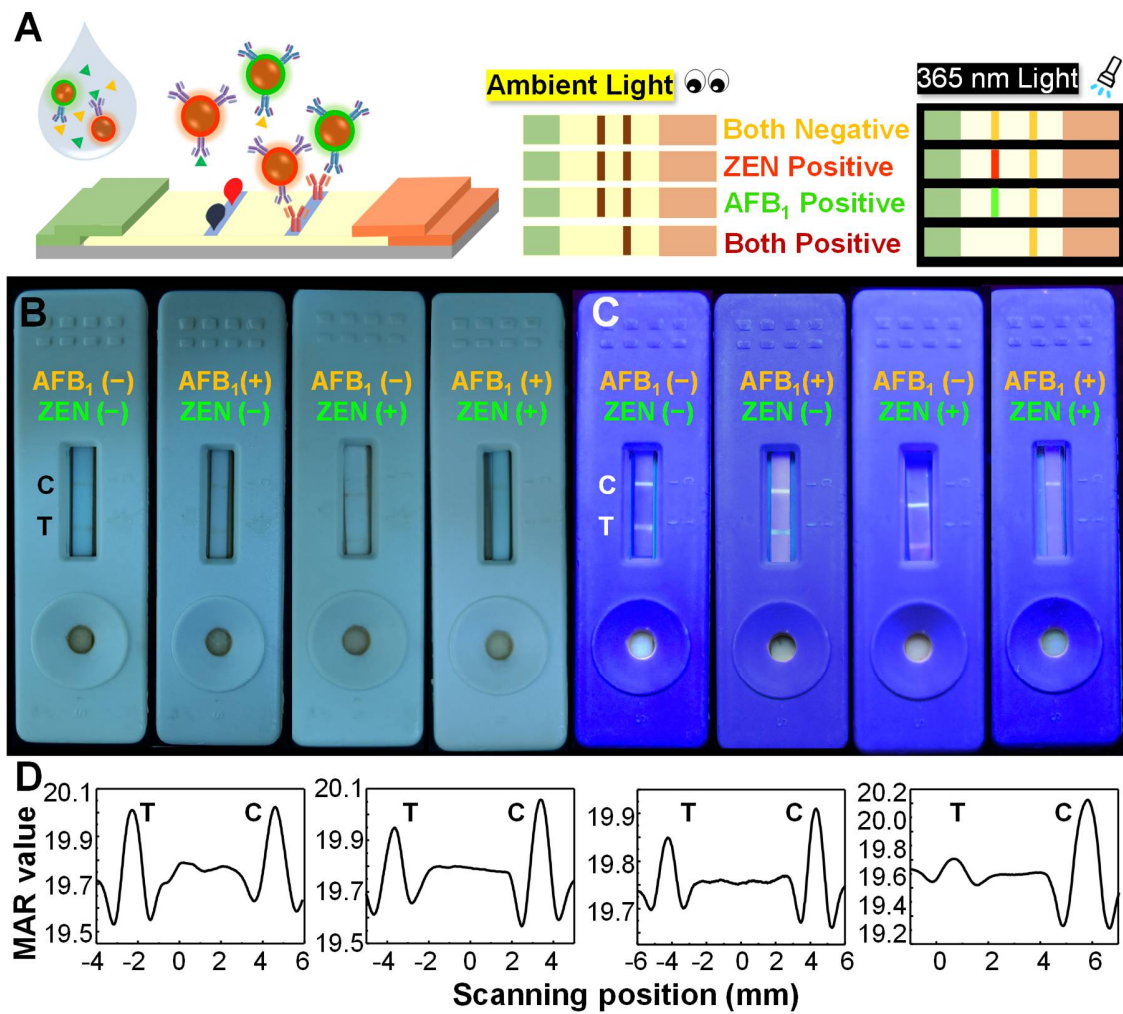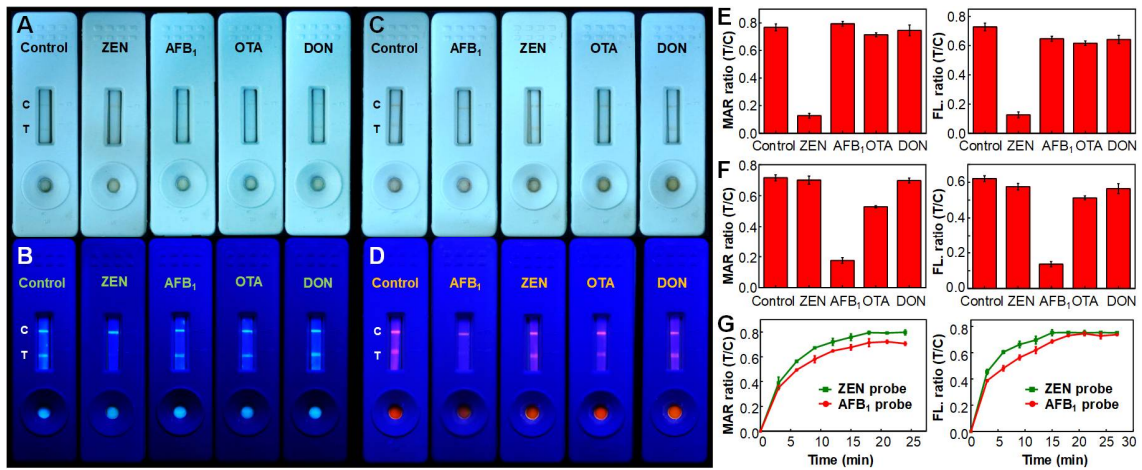
Supplementary Information

regulated by the Taiwan Food and Drug Administration.[4] As Table S1 outlines, ZEN and AFB$_1$ levels in fresh samples are either undetectable or fall below the detection threshold of the test strips. In contrast, the conventional HPLC method can identify much lower ZEN and AFB$_1$ levels in fresh corn and barley. However, the process involves complex instruments, lengthy procedures, and considerable time. In the case of stale samples, the concentrations determined by the test strips exhibit a high level of agreement with those determined by HPLC. This indicates that the bimodal ICTS based on MNP@Pdot is a practical approach for detecting ZEN and AFB1 in food. With suitable modifications to the probes and test lines, the target of interest can be expanded to include other mycotoxins.

Table S2. Comparison of this ICTS Platform with Other ICTS Methods. (NA: Not available).

Reporters	Target	LOD (ng/mL)	Linear Range (ng/mL)	Ref.
Aptamer-modified Au Nanoparticles	ZEN	20	5-200	[7]
Silica-coated quantum dots	ZEN	80	NA	[8]
Cy5-labeled aptamer	AFB$_1$	2.5	0.5-5000	[9]
Au nanoparticles	AFB$_1$	2.0	NA	[10]
This work	ZEN	4.87	0-100	
	AFB$_1$	2.15	0-25	

Supplementary Information

Figure S6. Enlarged image of Figure 1.

Figure S7. Enlarged image of Figure 2.

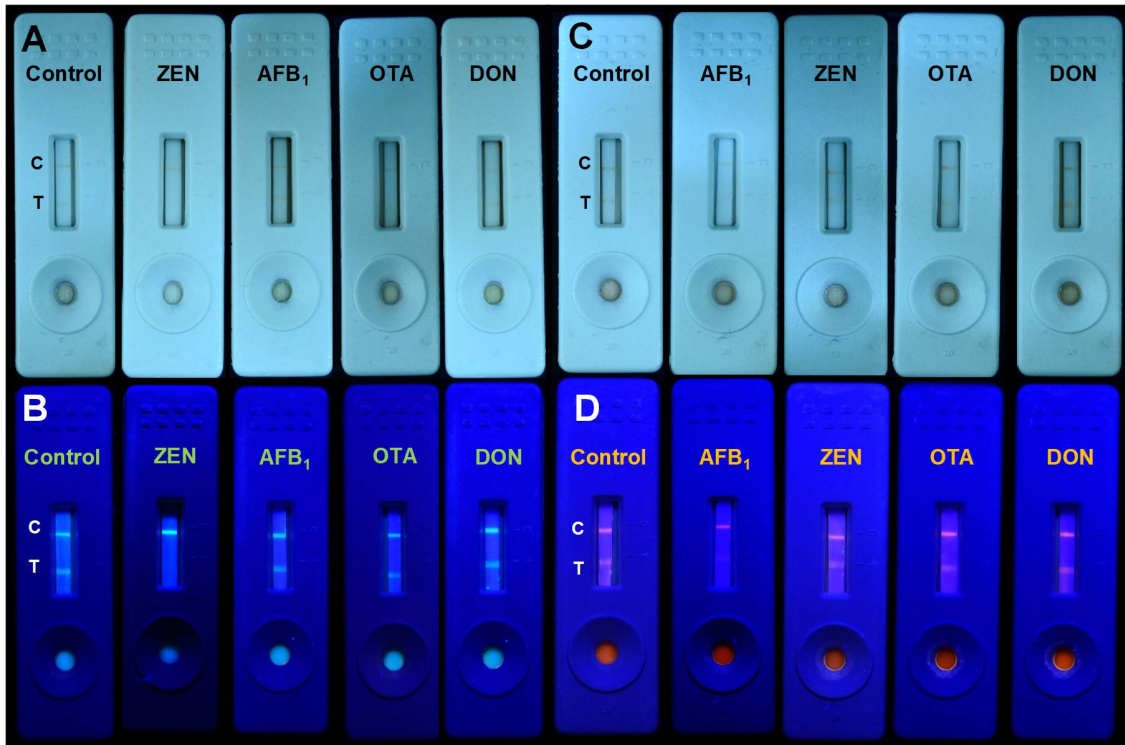# Supplementary Information

Figure S8. Duplicate data set 1 of Figure 1.
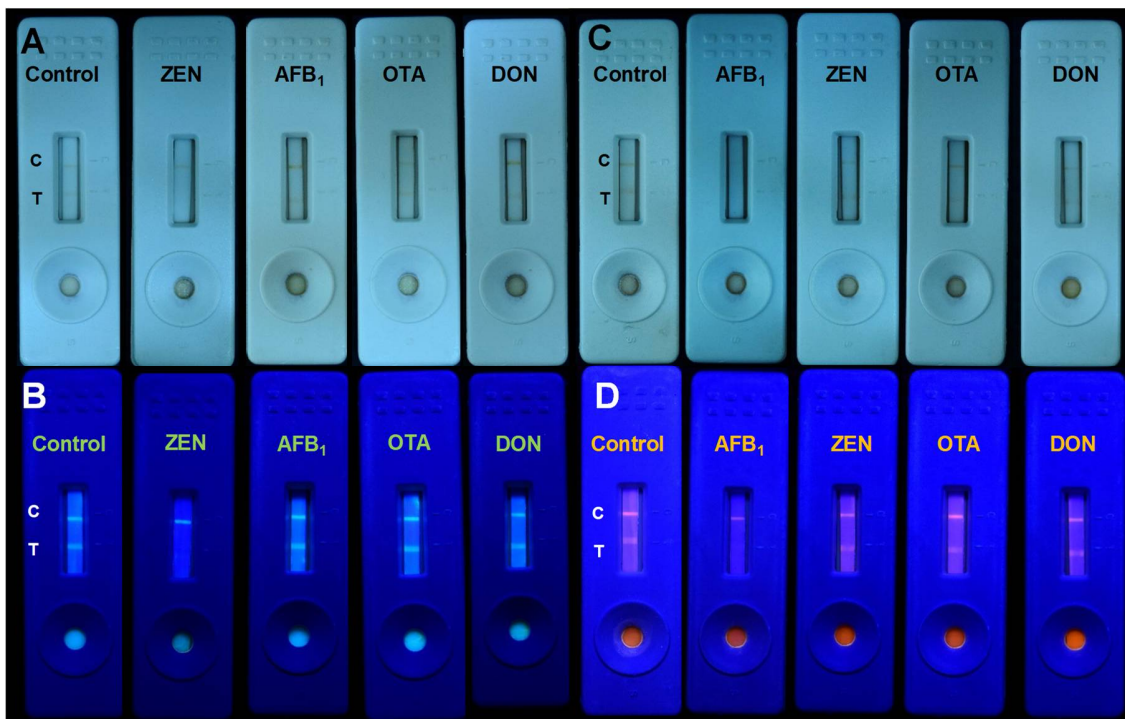
Figure S9. Duplicate data set 2 of Figure 1.
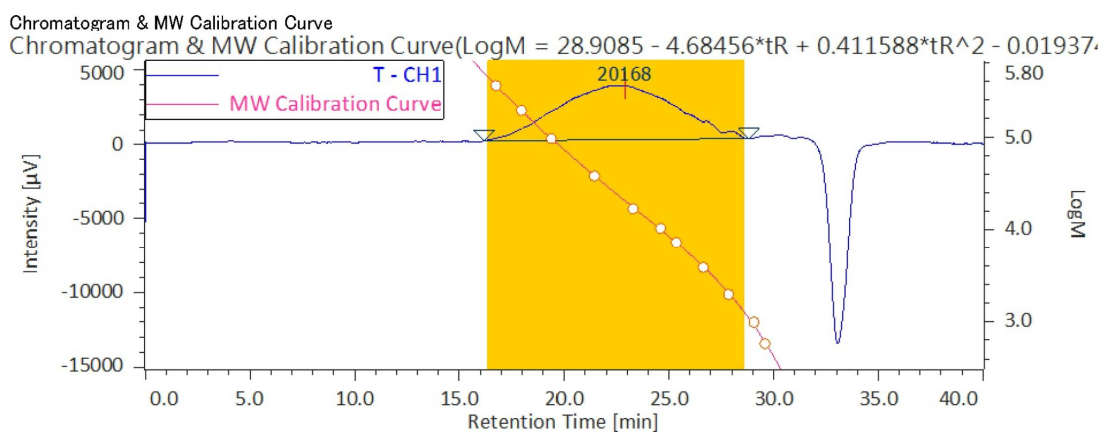
Supplementary Information

MW Calculation Results
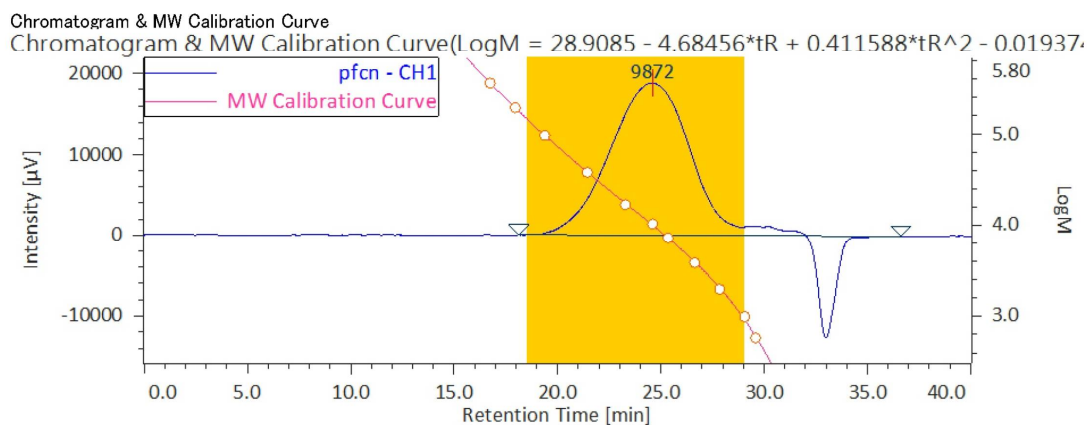
⟨ MW Calculation Results(Whole) ⟩

#	Range	CH	Mp	Mn	Mw	Mz	Mv	Mw/Mn	Mz/Mw	Range Value	Percentage	Warning
1	Whole	1	---	7681	13879	23814	13879	1.8069	1.7159	5004797	---	

Figure S9. Gel permeation chromatography (GPC) measurements of the PFCN polymer.

MW Calculation Results

⟨ MW Calculation Results(Whole) ⟩

#	Range	CH	Mp	Mn	Mw	Mz	Mv	Mw/Mn	Mz/Mw	Range Value	Percentage	Warning
1	Whole	1	---	13470	41239	101386	41239	3.0615	2.4585	1410076	---	Extrapolation

Figure S10. GPC measurements of the PFTC6FQ polymer.
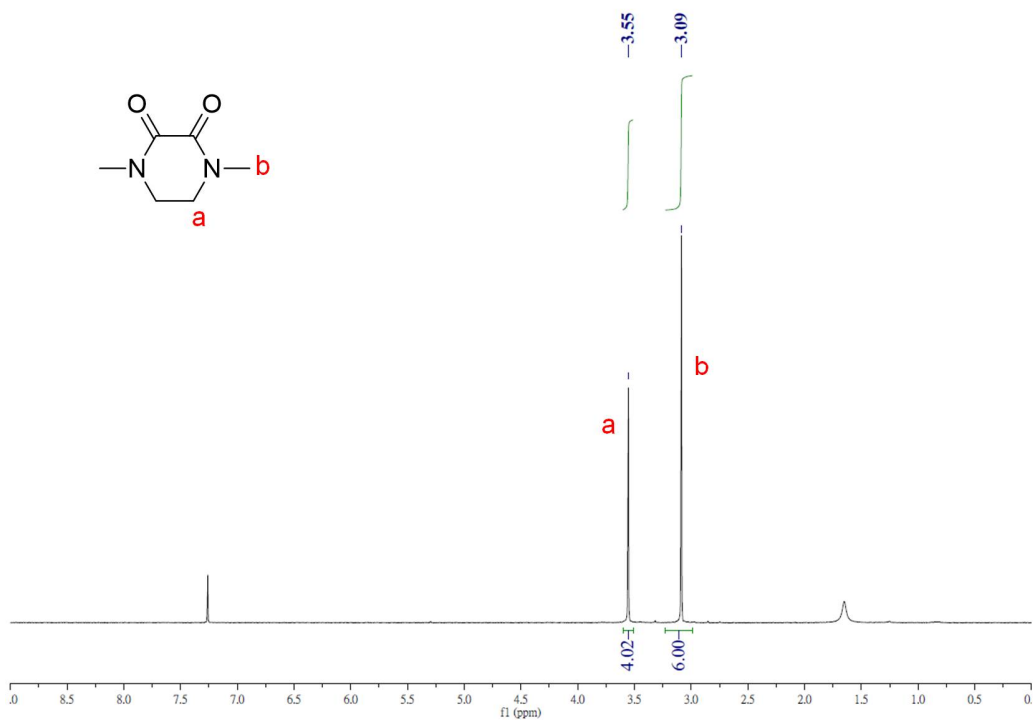
Supplementary Information
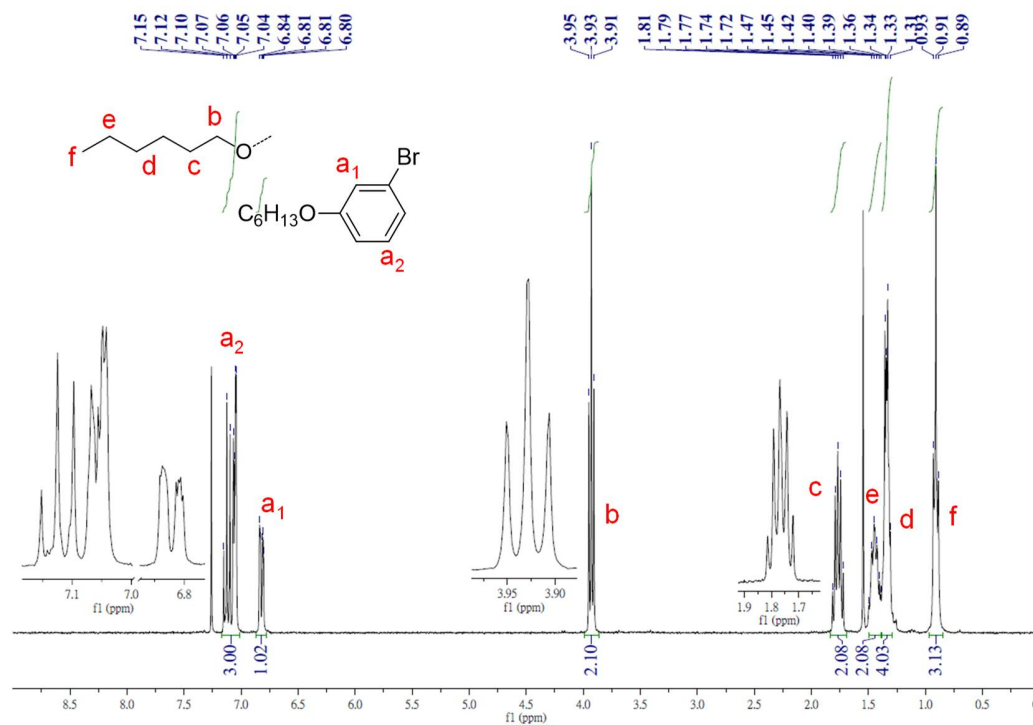
NMR Spectra

¹H NMR of **Compound 1**
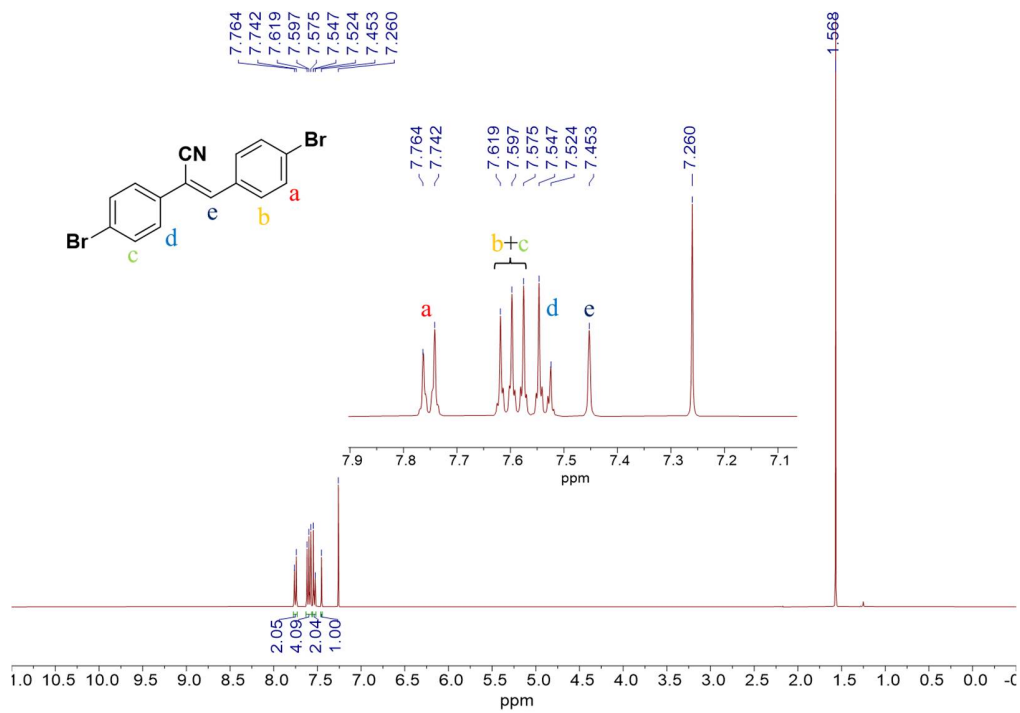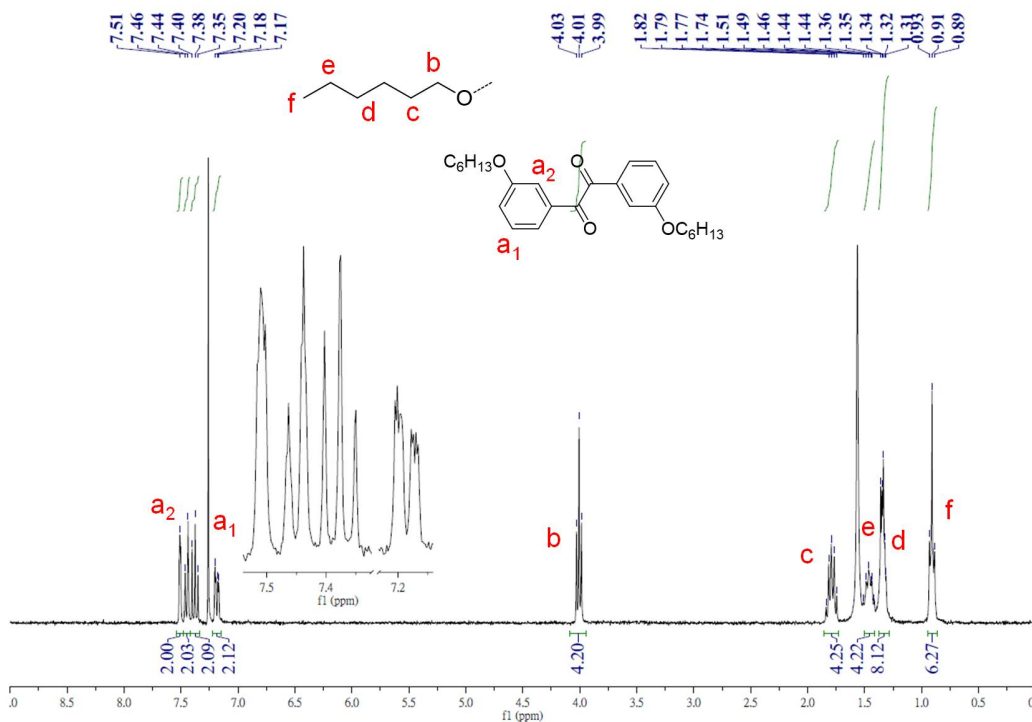

¹H NMR of **Compound 4**

Supplementary Information

^{1}H NMR of **Compound 5**

^{1}H NMR of **Compound 6**

Supplementary Information

^{1}H NMR of **Compound 8**
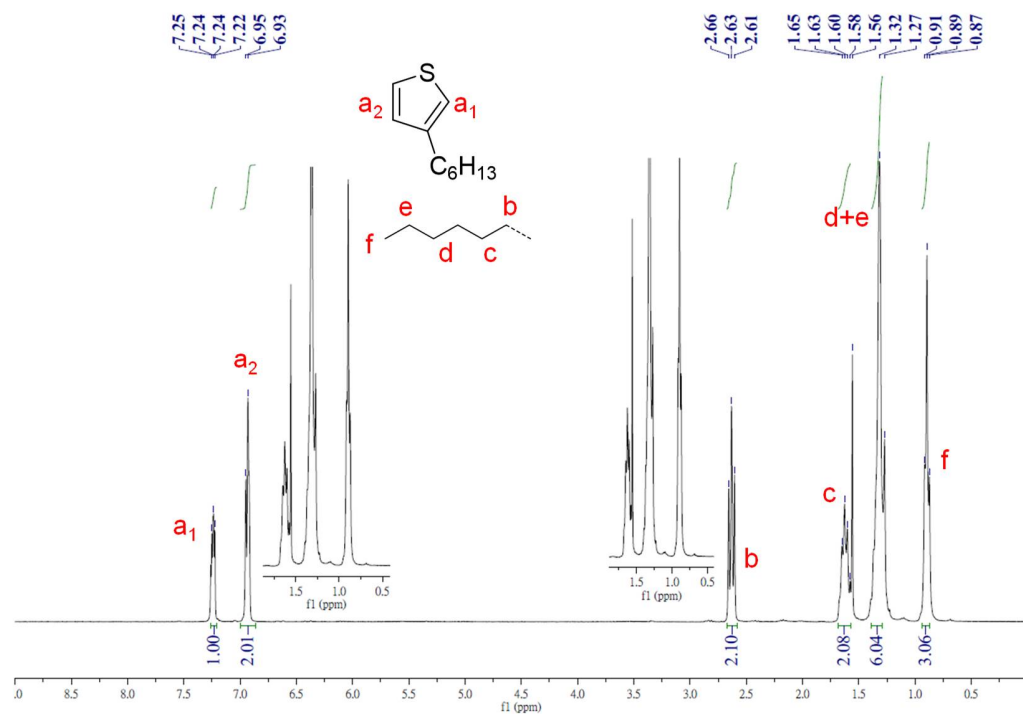
^{1}H NMR of **Compound 10**

Supplementary Information
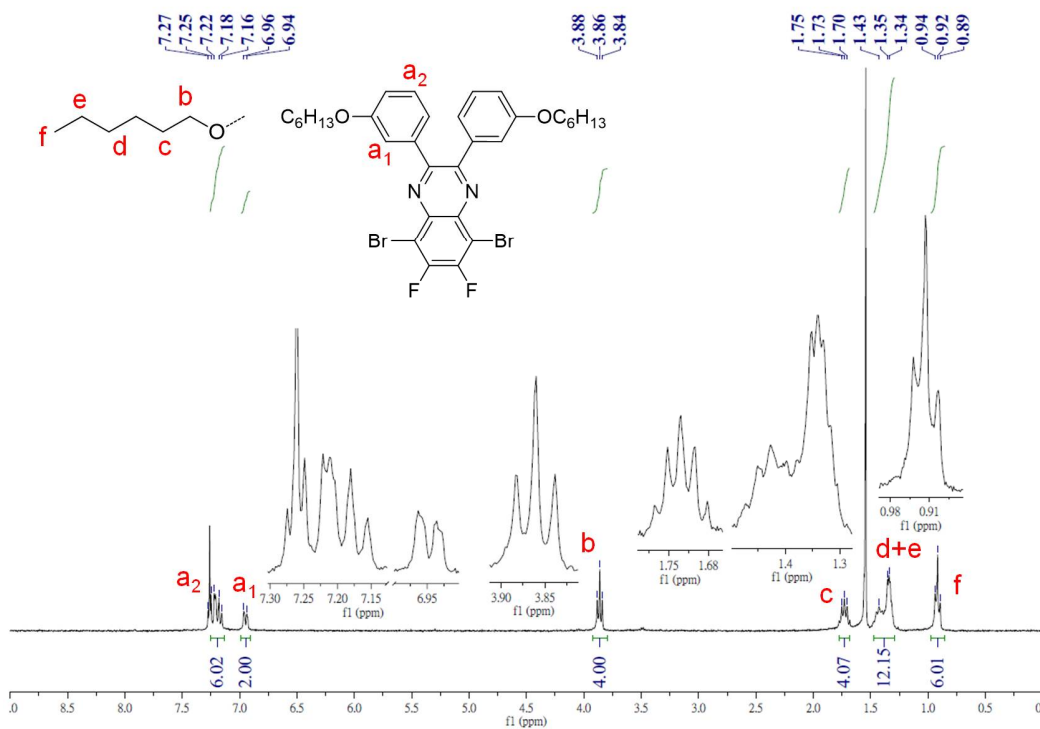
^{1}H NMR of **Compound 11**
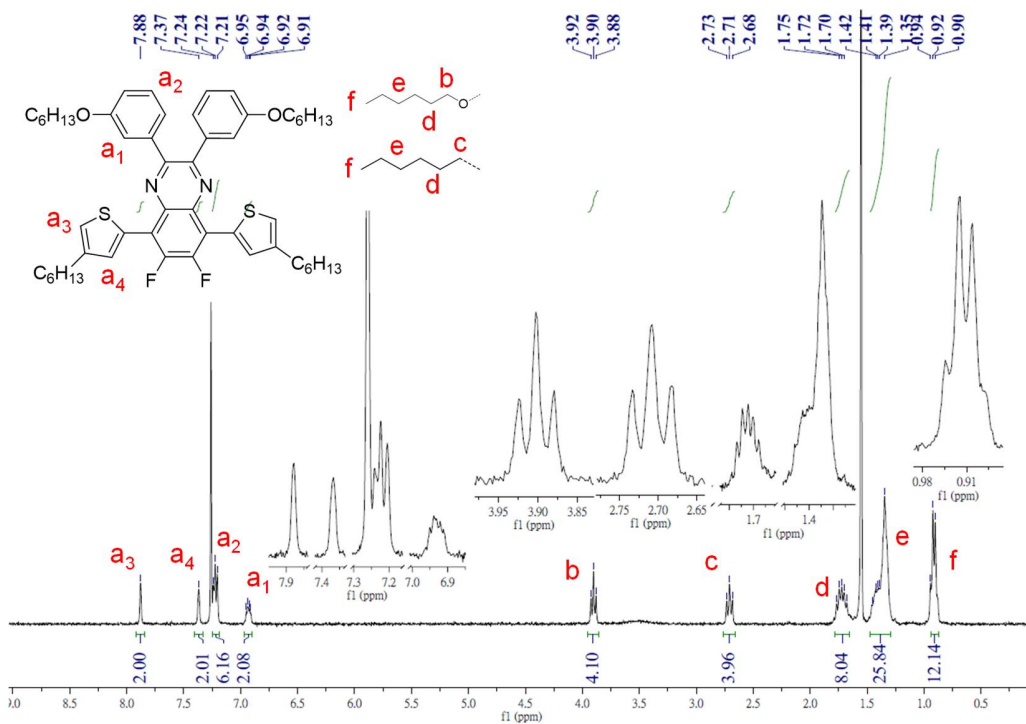
^{1}H NMR of **Compound 12**
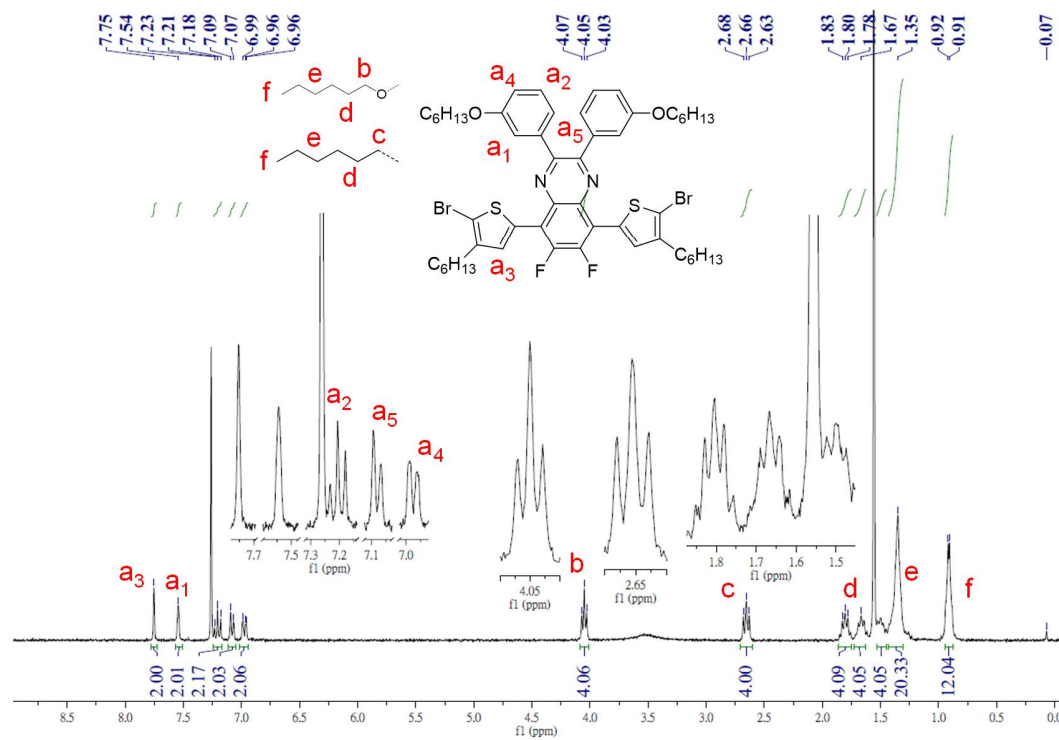
Supplementary Information

References:

[1]   C.-P. Chen, Y.-C. Huang, S.-Y. Liou, P.-J. Wu, S.-Y. Kuo, Y.-H. Chan, *ACS Appl. Mater. Interfaces* **2014**, 6, 21585.

[2]   H.-Y. Liu, P.-J. Wu, S.-Y. Kuo, C.-P. Chen, E.-H. Chang, C.-Y. Wu, Y.-H. Chan, *J. Am. Chem. Soc.* **2015**, 137, 10420.

[3]   X. Zhan, Y. Liu, X. Wu, S. Wang, D. Zhu, *Macromolecules* **2002**, 35, 2529.

[4]   Taiwan Food and Drug Administration. https://www.fda.gov.tw/upload/133/Content/2013091017150151016.pdf (accessed March 29, 2023).

[5]   R. T. LaBorde, B. O'Farrell, *IVD Technol.* **2002**, 8, 36.

[6]   J. Singh, A. Mehta, *Food Sci. Nutr.* **2020**, 8, 2183.

[7]   S. Wu, L. Liu, N. Duan, Q. Li, Y. Zhou, Z. Wang, *J. Agric. Food Chem.* **2018**, 66, 1949.

[8]   A. Foubert, N. V. Beloglazova, A. Gordienko, M. D. Tessier, E. Drijvers, Z. Hens, S. D. Saeger, *J. Agric. Food Chem.* **2017**, 65, 7121.

[9]   C. Zhu, G. Zhang, Y. Huang, S. Yang, S. Ren, Z. Gao, A. Chen, *J. Hazard. Mater.* **2018**, 344, 249.

[10]   B.-H. Liu, Y.-T. Hsu, C.-C. Lu, F.-Y. Yu, *Food Control* **2013**, 30, 184.